ChemComm

Accepted Manuscript

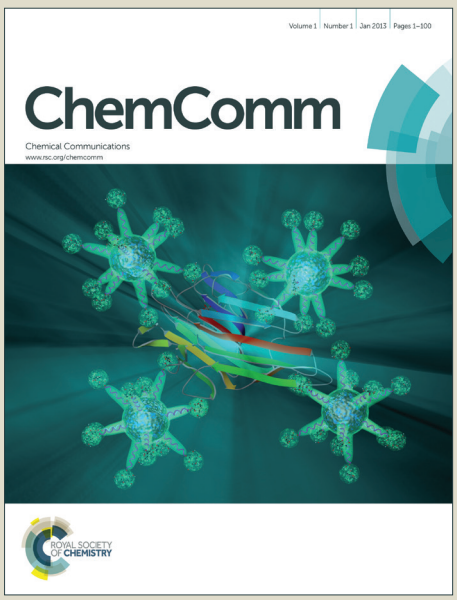

ROYAL SOCIETY OF CHEMISTRY

www.rsc.org/chemcomm

Journal Name

RSCPublishing

COMMUNICATION

Co-self-assembled Nanoaggregates of BODIPY Amphiphiles for Dual Colour Imaging of Live Cells

Cite this: DOI: 10.1039/x0xx00000x

Received 00th January 2012,
Accepted 00th January 2012

DOI: 10.1039/x0xx00000x

www.rsc.org/

Gang Fan,[a,b] Yao-Xin Lin,[b] Le Yang,[a] Fu-Ping Gao,[b] Ying-Xi Zhao,[b] Zeng-Ying Qiao,[b] Qiong Zhao,[b] Yun-Shan Fan,[b] Zhijian Chen,*[a] and Hao Wang*[b]

Co-self-assembled vesicular nanoparticles of two structurally comparable amphiphilic boron-dipyrromethene (BODIPY) dyes with dequenchable dual colour fluorescence were prepared for ratiometric imaging of live cells.

In recent years, the construction of fluorescence imaging probes by molecular self-assembly process is of great interest to the researchers in the interdisciplinary area of supramolecular chemistry and bioimaging.[1] By using building blocks such as functional dyes,[2] π-conjugated oligomers,[3] amphiphilic polymers,[4] graphenes,[5] metal complexes,[6] peptides,[7] *etc.*, a variety of supramolecular imaging nano-probes have been conveniently prepared. Moreover, the supramolecular strategy[8] provides effective pathways to improve the sensitivity of the fluorescent probes. In particular, the on/off switching of the fluorescence of imaging probes can be modulated by the control of aggregation and disaggregation of fluorophores to enhance the target-to-background ratio of the signals.[9] Nevertheless, imaging inaccuracy can also stem from the intensity fluctuation of excitation light, the probe concentration, inner filter effect, and other issues.[10] To minimize these perturbations, efforts have been devoted to the development of dual colour imaging probe systems containing different fluorophores which are able to generate insusceptible, self-calibrating emission signals.[11] To this end, the co-self-assembly of two or more functional dyes with distinct and dequenchable fluorescence signals could be a promising approach, but there is still a lack of exploration in this aspect.

Boron-dipyrromethene (BODIPY)[12] dyes have been widely used for bioimaging and sensing owing to their intense fluorescence, narrow emitting band, and high stability in physiological conditions. For biological applications, a large number of water-soluble BODIPY dyes[13] have been synthesized by attaching ionic groups or neutral oligo-ethyleneglycol chains at the dipyrromethene core. On the other hand, BODIPY-based amphiphiles carrying both hydrophilic and hydrophobic moieties have been reported to form fluorescent nanoparticles and elongated aggregates in aqueous media.[14] These aggregates display distinct optical properties from that of monomeric dyes, *e.g.* red-shifted near-infrared fluorescence[14a] or aggregation-induced emission enhancement,[15] which could be beneficial for their applications.

We here report the aqueous co-self-assembly of two structurally comparable BODIPY amphiphiles **1** and **2** with distinct emission colour (Scheme 1). Of particularly interesting, the fluorescence of both dyes is fully quenched in the co-assembled vesicular nanoparticles, but dequenchable upon the disassembly driven by solvent variation or cell uptake. Accordingly, the potential application of the nanoaggregates of co-assembled dyes **1** and **2** for dual colour imaging of live cells was examined.

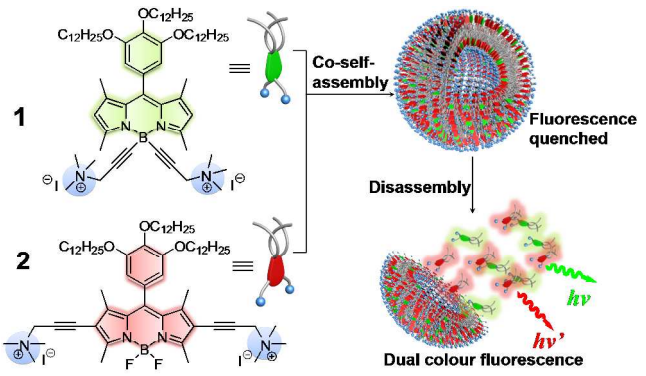

Scheme 1 Schematic illustration for the formation of fluorescence-quenched nanovesicular co-aggregates of **1** and **2** and the dequenching of fluorescence of both dyes upon the disassembly driven by cell uptake or solvent variation.

The BODIPY dyes **1** and **2**, both bearing a hydrophobic 3,4,5-tridodecyloxyphenyl substituent at the *meso*-position and two

hydrophilic quaternary ammonium groups attached to the boron atom (dye **1**) or the 2,6-positions (dye **2**), were synthesized in several steps starting from 3,4,5-tridodecyloxybenzaldehyde and fully characterized (see Electronic Supplementary Information). The UV/Vis absorption spectrum of BODIPY **1** in DMSO displayed absorption bands between 450 and 525 nm for the $S_0 \rightarrow S_1$ transition with λ_{max} = 501 nm (Fig. 1). For dye **2**, the λ_{max} was bathochromically shifted 37 nm as compared with that of **1**, indicating the electronic interactions between the 2,6-alkynyl substituents and the BODIPY core. For both compounds, the emission bands are approximately the mirror image of their $S_0 \rightarrow S_1$ absorption bands. The emission maxima are located at 510 nm for dye **1** and 558 nm for dye **2** in DMSO. The fluorescence quantum yields of **1** and **2** were determined to be 0.17 and 0.23 in DMSO, respectively.

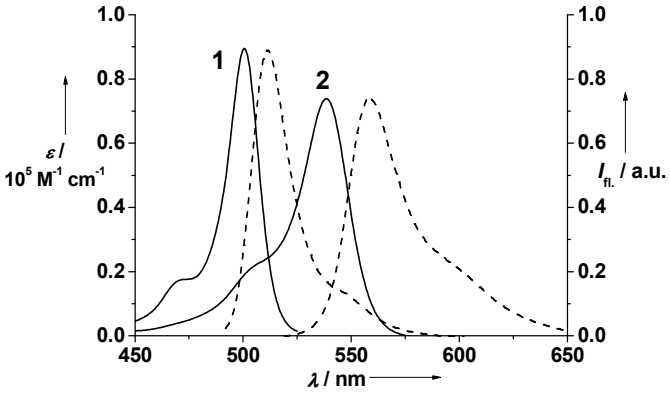

Fig. 1 UV/Vis absorption (solid lines) and fluorescence spectra (dashed lines) of dyes **1** and **2** in DMSO (λ_{ex} = 470 nm for **1** and λ_{ex} = 510 nm for **2**).

The UV/Vis absorption spectra of **1** and **2** in DMSO are typical for non-aggregated BODIPYs.[16] However, upon addition of the poor solvent water into the DMSO solutions of **1** or **2**, distinct absorption spectral changes were observed (Fig. S9-10†), which are highly indicative for the formation of aggregates of both dyes. On the basis of these observations, the co-self-assembly properties of dye **1** and **2** were further investigated DMSO-containing water. When the content of DMSO in solvent is greater than or equal to 63% (Fig. 2a), the UV/Vis absorption spectrum of **1/2** mixture ([**1**] = [**2**] = 2.5 × 10^{-4} M) can be interpreted as a simple sum of the spectra of molecularly dissolved BODIPY **1** and **2** and the $S_0 \rightarrow S_1$ transition bands of the two components can be easily distinguished. With decreasing DMSO content in the system, the two monomer bands gradually decrease and a new bathochromically shifted band with λ_{max} around 564 nm appears, indicating a well-defined transition from monomeric species to co-aggregates. The same transition was also observed in temperature-dependent spectroscopic studies (Fig. 2b) in water containing DMSO. With stepwisely decreasing the temperature from 60 °C to 5 °C, gradually increase of the aggregation band with λ_{max} = 564 nm was observed. In contrast, this aggregation band was not observed for pure **1** or **2** under same solvent or temperature variation. All these pronounced spectral changes indicate strong electronic interactions between chromophores and the formation of *J*-type co-aggregates of the BODIPY mixtures.

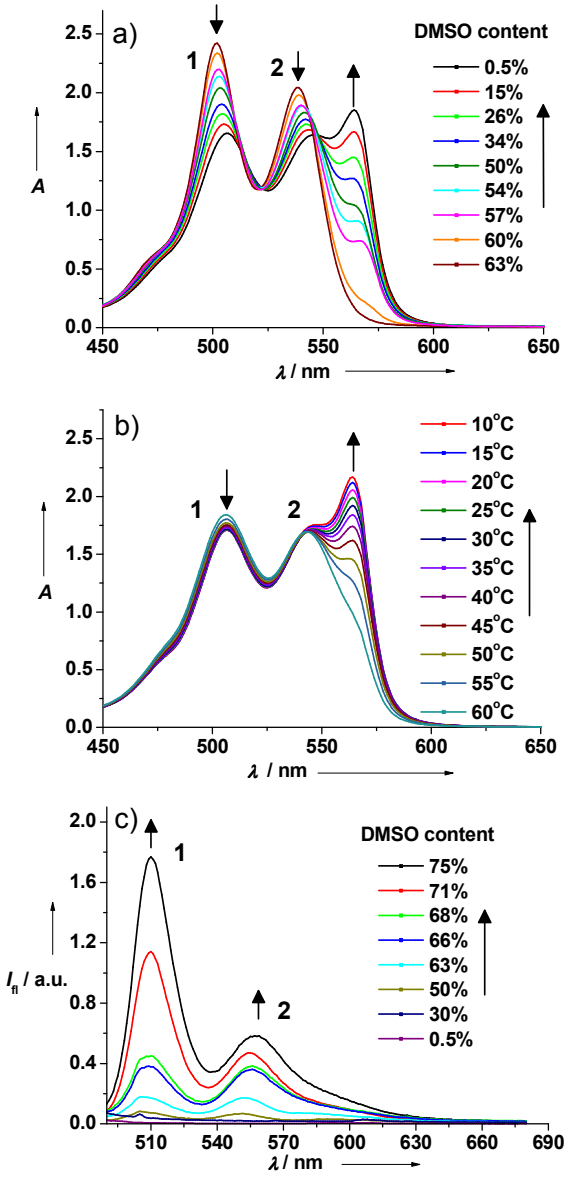

Fig. 2 (a) UV/Vis absorption spectra of **1/2** mixture ([**1**] = [**2**] = 2.5 × 10^{-4} M) in DMSO-containing water with decreasing DMSO content (63% to 0.5%, v/v). (b) Temperature-dependent UV/Vis absorption spectra of **1** and **2** ([**1**] = [**2**] = 2.5 × 10^{-4} M) in DMSO-containing water (0.5% DMSO, v/v) and the arrows indicate the spectra changes with increasing temperature. (c) Fluorescence spectra of **1/2** mixture ([**1**] = [**2**] = 2.5 × 10^{-4} M, λ_{ex} = 460 nm) in DMSO-containing water with increasing DMSO content (0.5% to 75%, v/v).

More interestingly, the fluorescence of both dyes was fully quenched when they co-aggregate in DMSO-containing water. The recovery of fluorescence of both dyes was observed when the co-assemblies of **1** and **2** were disaggregated by increasing the content of DMSO in solution (Fig. 2c). The dual colour fluorescence dequenching upon dissembling of the co-aggregates based on amphiphilic BODIPY **1** and **2** can be

considered as "turn on" fluorescence that could be used for cell imaging to increase the signal-to-noise ratio.

For the BODIPY amphiphiles **1** and **2**, their Israelachvili's packing parameters (or shape factors)[17] were estimated to be 0.8 and 0.9 respectively (see ESI). This result implies the formation of vesicular aggregates in the aqueous solution of co-assembled dyes **1** and **2** with various molar ratios. To verify this prediction, the co-aggregates of **1** and **2** were prepared by solvent-switch method[18] in DMSO-containing water (0.5% DMSO, v/v) and were visualized by transmission electron microscopy (TEM). For the co-aggregates with a molar ratio of [**1**]/[**2**] = 1:5, spherical hollow vesicles with a mean diameter of 110 nm were observed (Fig. 3a) in TEM study. The wall thickness of the vesicles is c.a. 10 nm, suggesting that the vesicle wall has a multiple-layered structure (length of c.a. 2.5 nm for **1** and c.a. 2.3 nm for **2** with fully extended alkyl chains from molecular modelling). Dynamic light scattering (DLS) studies for the self-assembled sample (Fig. 3b) indicated that the average hydrodynamic size of particles was 120 nm with a polydispersity index of 0.24. The nanomorphology of co-aggregates of **1** and **2** was also confirmed by tapping-mode atom force microscopy and scanning electron microscopy (Fig. 3c, S11,12†). Furthermore, the vesicular morphology was also observed for the co-aggregates of **1** and **2** with molar ratios of [**1**]/[**2**] = 1:3 and [**1**]/[**2**] = 1:1 in TEM studies (Fig. S12†). For the co-aggregates with 1:1 ratio of the dyes, a well-resolved lamellar structure was observed for the vesicle wall with a interlayer spacing of c.a. 5 nm, corresponding the thickness of a bilayer of the dyes.

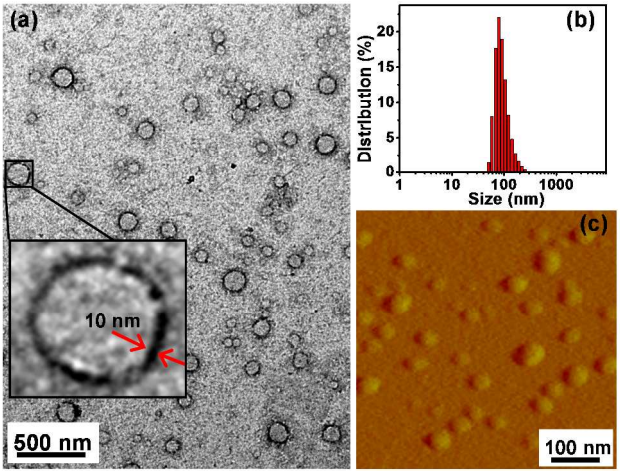

Fig. 3 (a) TEM images of co-aggregates of dye **1** and **2** ([**1**]/[**2**]= 1:5, [**2**] = 0.2 mg/mL). (b) Size distribution of the nanoaggregates by DLS measurements in DMSO-containing water (0.5% DMSO, v/v, [**1**]/[**2**]= 1:5, [**2**] = 0.2 mg/mL). (c) AFM amplitude image of vesicles ([**1**]/[**2**]= 1:5) on mica.

The defined vesicular morphology and the dequenchable fluorescence of the co-assembled nanoaggregates of **1** and **2** are beneficial for their application as probes in monitoring complex physiological processes. For such applications, the co-aggregation of dyes **1** and **2** was further examined in serum-free as well as serum-containing medium by UV/Vis spectroscopy and DLS. The results indicate that the dye co-aggregates are invulnerable in these medium (Fig. S13, S14†). The fluorescence of co-aggregated dyes remained quenched in above-mentioned medium. To use the nanoaggregates for dual-colour imaging of live cells, the suspension of nanovesicles ([**1**]/[**2**] = 1/5)[19] in DMSO-containing water (0.5%, v/v) was injected into culture medium containing human cervical cancer (HeLa) cells and studied by confocal laser scanning microscopy (Fig. 4). After incubation of two hours, a series of *Z*-stack images indicated good internalization of both dyes (Fig. S16†). Then the intracellular localization of BODIPYs was investigated by studying their co-localization with known organelle probes. The results showed that BODIPYs **1** and **2** partially co-localized with lysosome and mitochondria (Fig. S17-18†) while they mainly co-localized with Endoplasmic Reticulum (ER) Tracker, suggesting that the disaggregated dye molecules accumulated generally on ER in living cells (Fig. 4a-g).

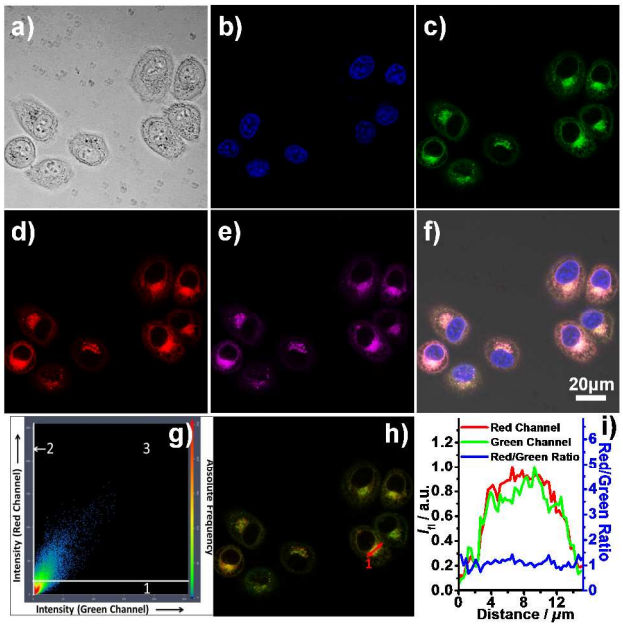

Fig. 4 Confocal microscope images of HeLa cells using Hoechst 33342, BODIPY vesicles ([**1**]/[**2**]=1/5), and ER Tracker Red as imaging probes. (a) Bright-field image. (b) Image for Hoechst. (c) Image for dye vesicles (channel 1, λ_{ex} = 488 nm, λ_{em} = 525 ± 25 nm). (d) Image for dye vesicles (channel 2, λ_{ex} = 543 nm, λ_{em} = 575 ± 25 nm). (e) Image for ER Tracker Red (channel 3, λ_{ex} = 594 nm, λ_{em} = 625 ± 25 nm). (f) Merged images. (g) Correlation plot of BODIPYs and ER Tracker Red emission intensities (Dual channel). (h) Merged image of channels 1 and 2. (i) Normalized intensity profile of ROIs across the red arrow in image (h).

From the intensity correlation plots (Fig. S19†), a high Pearson's coefficient of 0.66 and an overlap coefficient of 0.83 (0: no co-localization, 1: all pixels co-localized) were obtained respectively, confirming that the BODIPY co-aggregates can stain ER specifically. Typically a Pearson's coefficient above 0.4 is good.[20] In contrast, when using molecularly dissolved BODIPY **1** alone as imaging probe, the resultant Pearson's coefficient decreased to 0.18 (Fig. S20, Table S1†), implying the co-self-assembly of the two dyes plays a key role for the specificity of the imaging probes. When the dual-colour signal readout was evaluated by measuring the intensity ratio of green and red signals in region of interests (ROIs) (Fig. 4h), almost constant ratiometric intensity of the fluorescence was obtained, ensuring

the accuracy of imaging. In addition, the real-time confocal microscopic imaging studies indicated that the BODIPY co-aggregates remain fluorescence- quenched in the extracelluar space while it becomes highly fluorescent only inside the cells, thereby providing high target-to-background ratio of fluorescence signals (Fig. S21†). Furthermore, the cytotoxicity of the BODIPY dyes **1** and **2** was assessed with the cell counting kit-8 (CCK-8) assay. The viability of Hela cells incubated with increasing amounts (5 μM to 40 μM) of a PBS dispersion of dyes **1**, **2** and their co-aggregates remains essentially unchanged after 24 h incubation (Fig. S22†).

Conclusions

The co-self-assembly of two newly synthesized charged BODIPY amphiphiles **1** and **2** was demonstrated by spectroscopic and microscopic methods and nanovesicular co-aggregates of two dyes with various mixing ratio were obtained in aqueous solution. These fluorescence-quenched nanoaggregates can disassemble into fluorescent dye molecules with distinct emission bands upon solvent variation or cell uptake. Dual color and ratiometric fluorescence imaging of live-cells indicated that the disaggregated dyes are localized on the endoplasmic reticulum. With their unique hollow vesicular morphology, the co-assembled BODIPY nanoaggregates have the potential to be further modified for the intracellular delivery and real-time imaging.

Acknowledgements

We are grateful to the National Natural Science Foundation of China (No. 21176184), National Basic Research Program of China (973 Program, 2013CB932701), Program for New Century Excellent Talents by the Ministry of Education (NCET-09-0584), the 100-Talent Program of the Chinese Academy of Sciences, and Beijing Natural Science Foundation (2132053) for financial support for this work.

Notes and references

[a]School of Chemical Engineering and Technology and Collaborative Innovation Center of Chemical Science and Chemical Engineering (Tianjin), Tianjin University, Tianjin, 300072, China, E-mail: zjchen@tju.edu.cn
[b]CAS Key Laboratory for Biological Effects of Nanomaterials and Nanosafety, National Center for Nanoscience and Technology (NCNST) , 100190 Beijing, China, E-mail: wanghao@nanoctr.cn

† Electronic Supplementary Information (ESI) available: Synthesis and characterization of BODIPY dyes **1** and **2**, and additional results. See DOI: 10.1039/c000000x/

1 (*a*) H. Cabral, N. Nishiyama and K. Kataoka, *Acc. Chem. Res.*, 2011, **44**, 999; (*b*) E. Busseron, Y. Ruff, E. Moulin, and N. Giuseppone, *Nanoscale*, 2013, **5**, 7098; (*c*) M. J. Sailor and J.-H. Park, *Adv. Mater.*, 2012, **24**, 3779; (*d*) L. Wang, L. Li, Y. Fan and H. Wang, *Adv. Mater.*, 2013, **25**, 3888; (*e*) B. Godin, E. Tasciotti, X. Liu, R. E. Serda and M. Ferrari, *Acc. Chem. Res.*, 2011, **44**, 979.

2 (*a*) A. Palma, L. A. Alvarez, D. Scholz, D. O. Frimannsson, M. Grossi, S. J. Quinn and D. F. O'Shea, *J. Am. Chem. Soc.*, 2011, **133**, 19618; (*b*) D Zhang, Y.-X. Zhao, Z.-Y. Qiao, U. Mayerhöffer, P. Spenst, X.-J. Li, F. Würthner, and H. Wang, *Bioconjugate Chem.*, 2014, **25**, 2021; (*c*) B. Wang and C. Yu, *Angew. Chem. Int. Ed.*, 2010, **49**, 1485; (*d*) K.-R. Wang, D.-S Guo, B.-P. Jiang and Y. Liu, *Chem. Commun.*, 2012, **48**, 3644.

3 (*a*) I. Fischer, K. Petkau-Milroy, Y. L. Do.rland, A. P. H. J. Schenning, and L. Brunsveld, *Chem. Eur. J.*, 2013, **19**, 16646; (*b*) C. Zhu, Q. Yang, L. Liu and S. Wang, *Chem. Commun.*, 2011, **47**, 5524.

4 (*a*) M. C. L. Yeung, K. M. C. Wong, Y. K. T. Tsang and V. W.-W. Yam, *Chem. Commun.*, 2010, **46**, 7709; (*b*) Y. Ding, Y. Yi, H. Xu, Z. Wang and X. Zhang, *Chem. Commun.*, 2014, **50**, 2585.

5 C. S. Wang, J. Y. Li, C. Amatore, Y. Chen, H. Jiang and X. M. Wang, *Angew. Chem., Int. Ed.*, 2011, **50**, 11644.

6 (*a*) M. C. L. Yeung, K. M. C. Wong, Y. K. T. Tsang and V. W.-W Yam, *Chem. Commun.*, 2010, **46**, 7709; (*b*) R. Liu, J. Zhai, L. Liu, Y. Wang, Y. Wei, X. Jiang, L. Gao, H. Zhu, Y. Zhao, Z. Chai and X. Gao, *Chem. Commun.*, 2014, **50**, 3560

7 A. Laromaine, L. Koh, M. Murugesan, R. V. Ulijn, M. M. Stevens, *J. Am. Chem. Soc.*, 2007, **129**, 4156

8 H. Wang, S. Wang, H. Su, K.-J. Chen, A. L. Armijo, W.-Y. Lin, Y. Wang, J. Sun, K.-i. Kamei, J. Czernin, C. G. Radu and H.-R. Tseng, *Angew. Chem. Int. Ed.*, 2009, **48**, 4344.

9 (*a*) H. Kobayashi, M. Ogawa, R. Alford, P. L. Choyke and Y. Urano, *Chem. Rev.*, 2010, **110**, 2620; (*b*) K. Mizusawa, Y. Takaoka and I. Hamachi, *J. Am. Chem. Soc.*, 2012, **134**, 13386; (*c*) E. Nakata, Y. Yukimachi, Y. Nazumi, M. Uwate, H. Maseda, Y. Uto, T. Hashimoto, Y. Okamoto, H. Hori and T. Morii, *RSC Adv.*, 2014, **4**, 348.G; (*d*) Lukinavičius, L. Reymond, E. D'Este, A. Masharina, F. Göttfert, H. Ta, A. Güther, M. Fournier, S. Rizzo, H. Waldmann, C. Blaukopf, C. Sommer, D. W. Gerlich, H.-D. Arndt, S. W. Hell and K. Johnsson, *Nat. Methods* 2014, **11**, 731; (*e*) T. Yoshii, K. Mizusawa, Y. Takaoka and I. Hamachi, *J. Am. Chem. Soc.* **2014**, 136, 16635.

10 H. Lam, Y. Kostov, G. Rao and L. Tolosa, *Rev. Sci. Instrum.*, 2009, **80**, 124302-1.

11 (*a*) T. Guo, L. Cui, J. Shen, R. Wang, W. Zhu, Y. Xu and X. Qian, *Chem. Commun.*, 2013, **49**, 1862; (*b*) H. Yu, Y. Xiao, H. Guo and X. Qian, *Chem. Eur. J.*, 2011, **17**, 3179; (c) H. Kobayashi, Y. Koyama, T. Barrett, Y. Hama, C. A. A. Regino, I. S. Shin, B. -S. Jang, N. Le, C. H. Paik, P. L. Choyke, Y. Urano, *ACS Nano*, 2007, **1** , 258.

12 A. Loudet and K. Burgess, *Chem. Rev.*, 2007, **107**, 4891.

13 G. Fan, L. Yang and Z. Chen, *Front. Chem. Sci. Eng.*, 2014, **8**, 405.

14 (*a*) J.-H. Olivier, J. Widmaier and R. Ziessel, *Chem. Eur. J.*, 2011, **17**, 11709; (*b*) Y. Tokoro, A. Nagai and Y. Chujo, *Tetrahedron Letters*, 2010, **51**, 3451; (*c*) N. K. Allampally, A. Florian, M. Mayoral, C. Rest, V.Stepanenko and G. Fernández, *Chem. Eur. J.*, 2014, **20**, 10669.

15 S. Choi, J. Bouffard and Y. Kim, *Chem. Sci.*, 2014, **5**, 751.

16 F. Bergström, I. Mikhalyov, P. Hägglöf, R. Wortmann, T. Ny and L. B. -Å. Johansson, *J. Am. Chem. Soc.*, 2002, **124**, 196.

17 J. Israelachvili, *Colloids and Surfaces A: Physicochemical and Engineering Aspects*, 1994, **91**, 1.

18 J. Du and R. K. O'Reilly, *Soft Mater*, 2009, **5**, 3544.

19 Note that the ratio of [**1**]/[**2**] = 1/5 was chosen for the moderate size of the co-aggregates with narrow polydispersity, see ESI.

20 F. Cardarelli, D. Pozzi, A. Bifone, C. Marchini and Caracciolo G, *Mol. Pharmaceutics*, 2012, **9**, 334.

